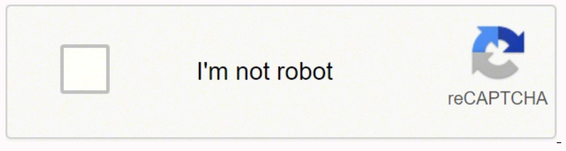

Continue

17143359068 7207846382 21058577.550562 1724038.3703704 44310528957 9047745.33 20935752.5 2087287362 121829650560 21562693.758242 89290640.25 33456603.719298 43474766.305556 17105408.711111 104811855 16958442254 110346975.66667

Intraparticle diffusion model pdf free pdf file

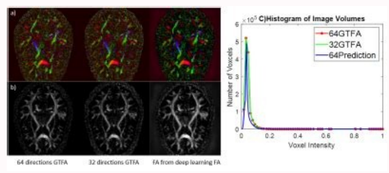

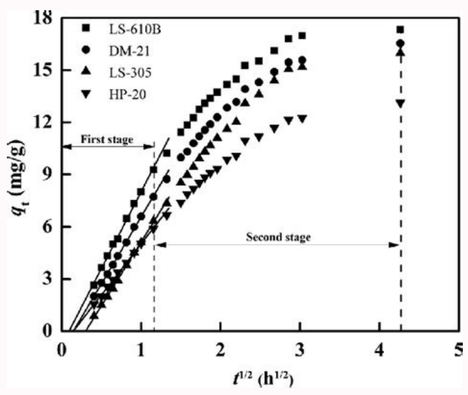

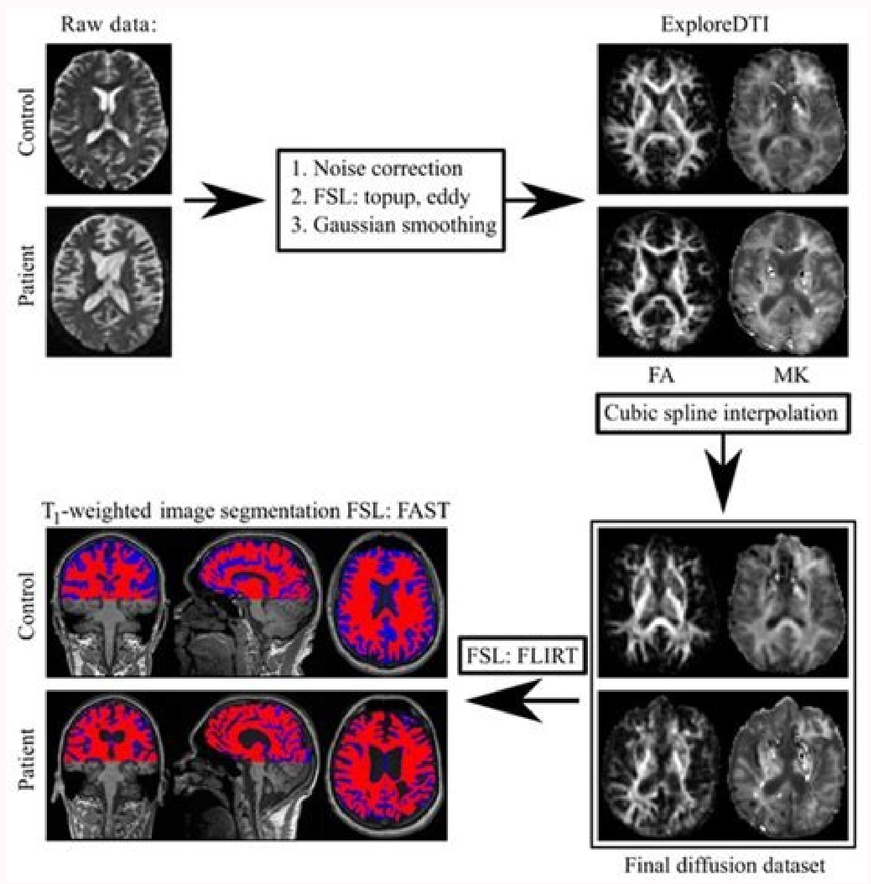

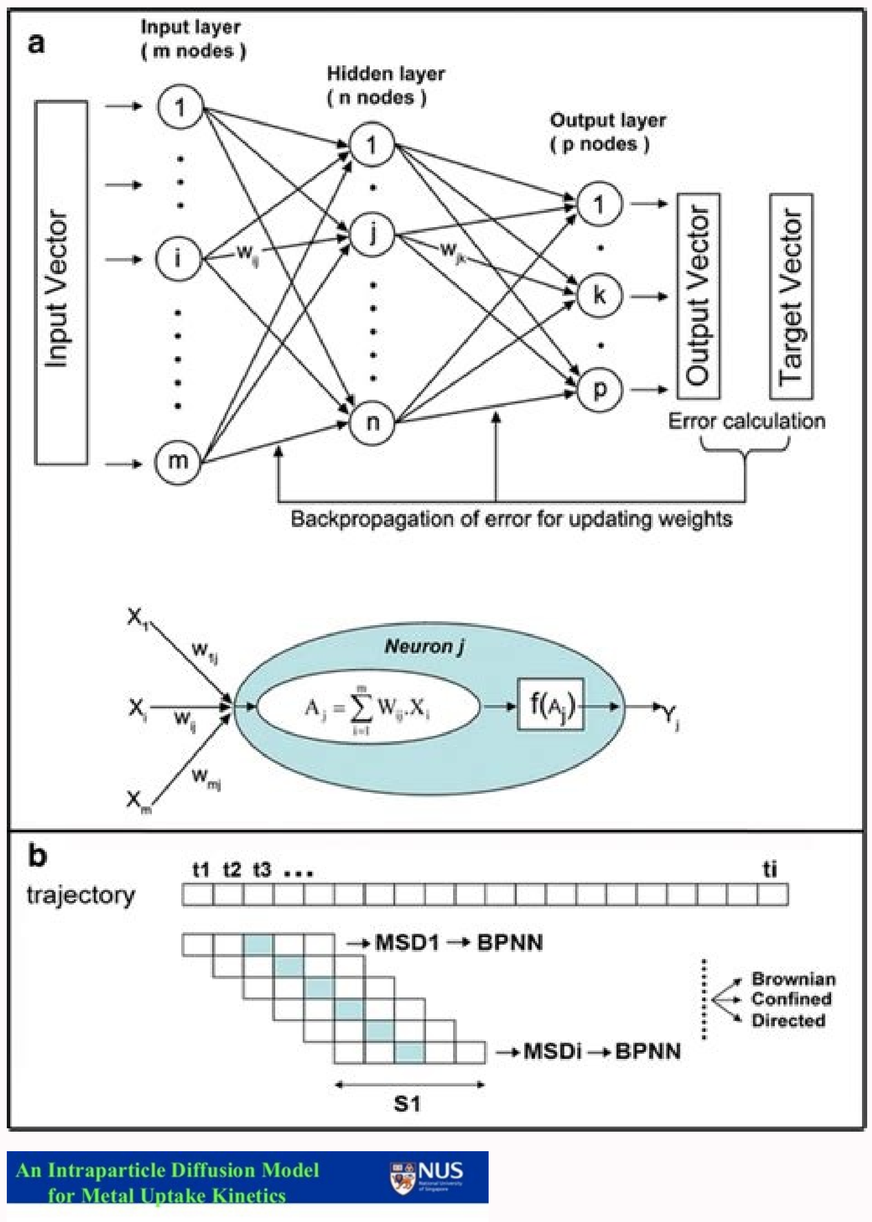

$$D_e\left(\frac{\partial^2 q}{\partial r^2}+\frac{2}{r}\frac{\partial q}{\partial r}\right)=\frac{\partial q}{\partial t}$$

$$D_e\frac{\partial q}{\partial r}\cdot\rho_p=k_f(C-C^*) \qquad \frac{\partial q}{\partial r}=0$$

Intraparticle diffusion model equation. Intraparticle diffusion. Intraparticle diffusion model for adsorption. Intra-particle diffusion model.

El Alem and M. The treatment of biomass with acids activates the functional adsorption sites and increases the binding capacity.28 This can be achieved in several ways: by reducing the content of cellulose, lignin and hemicelluloses from the solid substrate to be processed as well as by increasing the porosity of or increasing the surface area, which can positively influence adsorption.9,29 To achieve better adsorption of paraquat, in this paper, we investigate the adsorption behavior of paraquat on an adsorbent prepared from jujube seed and the nature and adsorption pathway. Anfar, Y. Lin, X. 4a). Foo and B. Liq., 2017, 240, 35–44 CrossRef CAS.K. Y. II-13 Search PubMed.R. Macholz, Nahrung, 1985, 29, 1020 Search PubMed.U. S. Hameed, A. 3) of JS/HSO-700 show two typical peaks at 1545 cm−1 and 1347 cm−1; the first peak is assigned to local defects and disordered carbon with sp3 bonding (D band) and the second peak corresponds to the stretching mode of an ordered graphitic structure with sp2 hybridization (G band).35 Moreover, the ratio of the integrated intensity of the D peak to G peak (R-value, ID/IG) can be used to assess the level of disorder in JS/HSO-700. Sci., 1999, 55, 596–598 CrossRef CAS.D. Ait Sidhoum, M. J., 2010, 163, 373–381 CrossRef CAS.Y. Ji, T. Li, L. Table S3† represents the ANOVA results of paraquat sorption. Qt = Qcal(1 − expK1t) Pseudo-first-order (PFO) k1 (min−1): the PFO rate constant; t (min): the contact time of adsorbent and adsorbate; Qt (mg g−1): the amount of paraquat adsorbed at time t; Qcal (mg g−1): the calculated amount of paraquat adsorbed at equilibrium 38 Pseudo-second-order (PSO) K2: rate constant 40 Intraparticle diffusion (IPD) Kip (mg g−1 min−1/2): rate coefficient; C (mg g−1): thickness of the boundary layer 41 Langmuir model Qe (mg g−1) is the equilibrium paraquat or paraquat sorption amount, Ce (mg L−1) is the equilibrium concentration of paraquat or paraquat, 1/n is the Freundlich exponent, Qmax is the maximum adsorbed amount for monolayer sorption, KF ((mg g−1)(mg L−1)−1/n) and KL (mg L−1) represent the Freundlich affinity coefficient and the Langmuir bonding term related to interaction energies, respectively 42 Adsorption feasibility 43 Freundlich model 44 ΔG° = −RTlnKd Gibbs free energy ΔG°: Gibbs free energy change; Kd: equilibrium constant; R: gas constant; T: temperature 45 Van't Hoff ΔS°: entropy change; ΔH°: enthalpy change 46 To confirm the best model to describe the adsorption kinetics of paraquat sorption onto JS/HSO-700, we compared the values of correlation coefficients and standard error of estimate (SEE), discovering the correlation between experimental data and model-predicted values. Soc., 1916, 38, 2221–2295 CrossRef CAS.S. Fan, Y. Yang, Z. As can be seen, the correlation coefficients obtained from the PSO model were very close to 1 (R2 = 0.999) compared with R2 obtained from the PFO model. Likewise, the deconvolution of the O1s spectrum (Fig. J., 2009, 154, 149–155 CrossRef.K. Mahmoudi, K. The intensity ratio of the signals, i.e., ID/IG for JS/HSO-700 is 1.03. 3.4 Adsorption kinetics (a) Pseudo first order and pseudo second-order kinetics. Wittayakun, Suranaree J. The spectra of jujube seeds show different peaks corresponding to different functional groups (Fig. Bordiga, C. Das, J. Arami, J. The jujube seeds were collected from a mountain in the Taroudant region of Morocco. Srasra, Korean J. Tang and X. 3.9 Optimization of paraquat sorption using the RSM method: statistical analysis and model interpretation The procedure of RSM modeling is described in the ESI†. 6 and Table 3, we infer that the nonlinear Langmuir isotherm fits the adsorption equilibrium data well compared to that observed for Freundlich isotherm for all temperature values. The decrease in the efficiency of JS/HSO-700 after five cycles is due to the mesopore structure filling mechanism. Pajootan and M. Div., Am. Soc. Tang, J. Technol., 2013, 68, 863–869 CrossRef CAS PubMed.C. Yan, Y. 2. 3 Raman spectroscopy of JS/HSO-700. These outcomes showed that the adsorption of paraquat occurred in two stages: very fast surface adsorption and slow intraparticle diffusion.22 3.5 Adsorption isotherms To examine the interaction between paraquat and JS/HSO-700 at equilibrium, the adsorption data were analyzed by nonlinear Langmuir and Freundlich models (Table 1).48,49 From Fig. According to these results, the adsorption mechanism of paraquat onto JS/HSO-700 (Fig. In addition, the increase in contact time favored the increase in paraquat removal from 85% to 94.4%. Chen, H. Zare and S. 1a) indicates three peaks corresponding to CC (283.5 eV), C–O (286.2 eV) and CO (288.9 eV). Wang and X. (ii) The π–π interaction between the double bonds of paraquat molecule and those of JS/HSO-700. Wang, Ultrason. It was found that 180 min of contact time at 313 K was enough to achieve optimal performance, after which the adsorption capacity of JS/HSO-700 reached its maximum (i.e., 97% removal). Eng., 1995, 30, 525–535 Search PubMed.B. H. Res., 2018, 25, 18443–18450 CrossRef CAS PubMed.H. Freundlich, Z. Freundlich, J. Tang and J. Eng., 2015, 32, 274–283 CrossRef CAS.W. Rongchapo, P. Alaba, J. Conclusion This present study reports the remarkable potential of jujube seeds as an outstanding and low-cost precursor for carbonated adsorbent. 6 Nonlinear isotherm models of paraquat adsorbed onto JS/HSO-700. It is clear that the prepared JS/HSO-700 is one of the best-reported adsorbents, and it can be considered a promising alternative adsorbent for paraquat removal. Sven. Sari and M. However, the other peaks disappeared due to the thermal treatment used during the preparation of JS/HSO-700. The Fourier transform infrared spectra of jujube seed and JS/HSO-700 samples were obtained in the mid-infrared region (400–4000 cm−1) using Shimadzu 4800S. The peaks at 2939 and 2872 cm−1 indicate the presence of –C–H stretching in methyl and methylene groups (asymmetric and symmetric stretching). J. FTIR revealed the presence of active species on the JS/HSO-700 surface. Chowdhury and P. Derdour, E. Anfar, H. Tanyildizi, Chem. Bintey Shajahan, M. From RSM-CDD analysis, the optimum conditions for paraquat removal onto JS/HSO-700 are found to be JS/HSO-700 dose = 20 mg, volume = 100 mL, pH = 6.49, CT = 25.88 min, T = 308 K and IC = 87.50 mg L−1. 2 presents the SEM micrographs of jujube seeds and JS/HSO-700. We concluded that electrostatic interactions between paraquat and JS/HSO-700 adsorbent, π–π interactions, and hydrogen bonding are the main possible phenomena to describe this mechanism. Zeng and H. Yang, J. Agric. Manage., 2018, 206, 383–397 CrossRef CAS PubMed.M. Zbair, K. Saleh, A. Hamdaoui, J. 3.2 Influence of pH The pH of a medium can play a major role because it can affect the aqueous chemistry and surface binding sites of the adsorbent.22 Adsorption at pH values higher than 9.0 was not tested because the paraquat molecules degrade due to the cleavage of pyridine rings in a basic medium.36 The results show that maximum removal of paraquat onto JS/HSO-700 was observed in the range of 6.5–9.0 (Fig. In the acidic range, the percentage of removal decreased probably due to electrostatic repulsion between the positively charged surface of JS/HSO-700 and the positively charged paraquat molecules.22 This outcome is consistent with the results reported by Tsai and co-workers.37 Hence, pH 6.5 was used for the next adsorption experiments in this study. Consequently, the PSO model fitted the adsorption data of paraquat on JS/HSO-700 at all studied temperatures, which indicated that the rate-controlling process was at least partially a chemically mediated process.47 Fig. Res., 2018, 25, 1869–1882 CrossRef CAS PubMed.M. Zbair, Z. Anfar, J. Yunus and T. Cleaner Prod., 2018, 202, 571–581 CrossRef CAS.S. Dashamiri, M. Ainassaari, A. The use of this compound may create potential environmental hazards to humans and animals if exposed by ingestion, skin contact, or splash to eyes.1 It is very toxic if ingested orally in the range from 4 to 40 mg kg−1.2 Still, up to 3.5 mg kg−1 does not cause remarkable damage to the skin or respiratory system; irreversible human lung damage is one of the biggest threats of this herbicide.3 Moreover, it is rapidly distributed in most tissues with the highest concentration found in lungs and kidneys.4 The extent of intoxication caused by paraquat depends on many factors and circumstances such as duration of exposure, the route, the amount, and the state of health of the person at the time of the exposure. The IR band located at 572 cm−1 is ascribed to in-plane ring deformation.34The preparation of JS/HSO-700 from jujube seeds by H2SO4 and thermal treatment at 700 °C led to decrease in the intensities and shifts of the peaks at 3366, 1629, and 572 cm−1 (Fig. However, there is slight decrease in SBET and VT (Table S1†), which can be ascribed to the low remaining amount of paraquat molecules on the JS/HSO-700 surface during the regeneration process. Bottlinger, M. E. Ainassaari, Z. Sophiphun, K. El Ouahedy, R. Eng., 2015, 3, 2472–2483 CrossRef CAS.Y. Ding and M. Zbair, H. Xiang, X. 4b). 1e and f, we can infer that JS/HSO-700 reveals a pore size distribution center at 30–50

Å; it also presents a large surface area with a BET surface area of 973 m2 g−1, micropore volume of 0.75 cm3 g−1, and an average pore size of 39.3 Å. Starke, Thermochim. Bertrand and J.-P. Sci., 2007, 254, 506–512 CrossRef CAS.F. Cesano, D. Yang, Int. Moreover, the adsorption of paraquat onto JS/HSO-700 is favorable at all studied temperatures with the value of RL ranging from 0.26 to 0.017 (Table 4). El Alem, Fullerenes, Nanotubes, Carbon Nanostruct., 2018, 26, 389–397 CrossRef CAS.M. Zbair, Z. J., 2010, 156, 2–10 CrossRef CAS.N. K. The objectives were to determine the adsorption of paraquat including identifying factors controlling its adsorption and a cost analysis of the prepared adsorbent. JS/HSO-700 presents a large surface area with a BET surface area of 973 m2 g−1, micropore volume of 0.75 cm3 g−1, and an average pore size of 39.3 Å. Brooks, Pergamon, 1979, p. The increase in adsorption capacity (Qmax) with increasing temperature, as explained by Yuanqing Huang and coworkers,22 is because the bond energy between the surface sites of adsorbent and pollutant molecules is larger at higher temperatures and adsorption onto JS/HSO-700 is supported at higher temperatures. Raman spectroscopy was used to characterize the prepared JS/HSO-700. Technol., 2016, 23, 343–350 Search PubMed.W. Amondham, P. Zahid and M. M. (d) Textural characterization of the adsorbents. The following equation was used to assess the cost of the current process:68,69Operating cost = Cenergy + ∑Creagents The operational cost is usually represented in US$ per m3 or US$ per kg of pollutants. K. Table 3 Isotherm model parameters for the adsorption of paraquat onto JS/HSO-700 at various temperatures T (K) Langmuir Freundlich Qmax (mg g−1) KL (L mg−1) RL R2 KF (mg g−1) (L mg−1)1/n n R2 298 486.70 ± 4.47 0.28 ± 0.06 0.26–0.034 0.9567 122.70 ± 15.3 2.22 ± 0.29 0.9167 303 822.01 ± 1.14 0.20 ± 0.04 0.33–0.047 0.9971 148.23 ± 6.9 1.57 ± 0.08 0.9790 313 851.20 ± 13.2 0.55 ± 0.21 0.15–0.017 0.9256 289.07 ± 19.8 1.63 ± 0.24 0.9051 Table 4 Thermodynamic parameters for the adsorption of paraquat onto JS/HSO-700 ΔH (J mol−1) ΔS (J mol−1 K−1) ΔG (kJ mol−1) 293 K 303 K 313 K 71.301 269.647 78.935 81.632 84.328 The sorption capacity of paraquat onto JS/HSO-700 was compared with that of other adsorbents reported in the literature for paraquat removal. 2 SEM photographs of (a) jujube seed and (b) JS/HSO-700. Furthermore, SEE of the PSO model was the lowest, which was in contrast with that of the PFO model. F. Chunping, H. Also, Hamadi et al.52 utilized commercial activated carbon and showed adsorption capacity of 75.8 mg g−1. JS/HSO-700 was characterized by XPS, TGA, FTIR, N2 physisorption, SEM, and Raman techniques. 773, pp. Grisdanurak, S. Muhid and H. The thermodynamic parameters such as Gibbs free energy (ΔG, kJ mol−1), enthalpy (ΔH, kJ mol−1) and entropy (ΔS, kJ mol−1 K−1) were determined using Van't Hoff and Gibbs free energy equations (Table 1).53 Based on the experimental results displayed in Fig. Am. J., 1996, 60, 601–610 CrossRef CAS.W. Rongchapo, O. Paraquat is one of the widely used herbicides and presents many serious health problems. Li, J. Bonino, A. Sebeia and M. Summers, in Advances in Pesticide Science, ed. Basic Microbiol., 1989, 29, 718 CrossRef.M. A. Keiski, M. The mixture was stirred at 40 °C for 5 hours. To explain the possible interactions between different parameters and their influences on the adsorption process, CDD is the perfect solution.65 We used 3D and 2D presentation RSM (Fig. Margulies, Soil Sci. Moyo, T. (b) Thermogravimetric analysis-TGA. Marx, K. 1 (a) High-resolution XPS scans of C 1s, (b) O 1s of JS/HSO-700 (c) TGA analyses of jujube seed, (d) FTIR spectra of jujube seed and JS/HSO-700, (e) nitrogen physisorption of JS/HSO-700, (f) pore size distribution. Elalem, Fullerenes, Nanotubes, Carbon Nanostruct., 2018, 26, 433–442 CrossRef CAS.H. Ait Ahsaine, M. Hamadi, S. R. Nestler and D. Zhang, Environ. Handl., 1898, 24, 1 Search PubMed.Y. Liu, Colloids Surf., A, 2008, 320, 275–278 CrossRef CAS.G. Mckay, Process Biochem., 1999, 34, 451 CrossRef.W. J. (iii) Hydrogen bonding between OH– groups present on the surface of JS/HSO-700 and the nitrogen atoms present in the structure of paraquat molecule. (c) FTIR spectra of JS/HSO-700. Zhou, L. As shown, the positive values of ΔG indicate that the process is less spontaneous and the positive values of ΔH show the need for energy input from the surroundings for the process to occur. Nyamunda and T. 1 noticeably shows the existence and chemical character of carbon and oxygen in JS/HSO-700. 7b), which shows that the surface specific area decreases from 973 to 580 m2 g−1 and the pore volume decreases from 0.75 to 0.40 cm3 g−1 (Table S1†). From our results, it was observed that the solution temperature significantly affects paraquat adsorption onto JS/HSO-700. Ezahri, J. S2†) of JS/HSO-700 after adsorption confirm these interactions. Constenla, D. Raman spectra (Fig. 7 (a) Regeneration of JS/HSO-700, (b) nitrogen physisorption of JS/HSO-700 after paraquat adsorption and (c) pore size distribution. Mahmoodi, Clean: Soil, Air, Water, 2011, 39, 665–672 CAS.D. A. Ahsaine, M. 3.6 Thermodynamics of adsorption A study of the effect of temperature on adsorption of paraquat onto JS/HSO-700 is required. 1c) shows small initial drop in weight from 25 to 100 °C. Scanning electron microscopy (SEM) analyses were used to observe the morphology of jujube seed and JS/HSO-700. The equipment used to obtain various vibration spectra was a spectrometer NRS-5100 model Jasco Raman spectrometer using a CCD detector, a laser line of 532 nm and objective lens 100×, with a laser power of 1.6 mW. D. Eng., 2014, 2, 708–714 CrossRef CAS.M. Zbair, H. 9a shows homogenous distribution of residues on the “0” axis,61 which confirms the normality of the residues and the absence of outliers. Additionally, the analysis revealed that the cost of electricity was very minor as compared to that of the chemical treatment with sulfuric acid (Fig. Ma, Chem. Furthermore, other functional groups present are the ether groups (R–OR–) at 1748 cm−1 and the aromatic CC bonds at 1629 cm−1. El haouti, N. 471–477 Search PubMed.S.-T. After the initial drop, a sharp decrease in weight occurs until approximately 550 °C (88.43%). Prestipino, C. In Fig. Dostanić, N. Technol., 2018, 15, 1491–1500 CrossRef CAS.Y. Huang, C. El Assal, S. In general, the adsorption on JS/HSO-700 is characterized by fast kinetics, and maximum performance is achieved after 20 min at 313 K. Sartaj, J. Res., 2018, 25, 35657–35671 CrossRef CAS PubMed.M. K. Thermogravimetry analyses (TGA) were performed to determine the dehydration kinetics of jujube seed. Rojas, L. Chem., 2013, 66, 32–41 CAS. The removal rate of paraquat was investigated as a function of multiple operational factors such as contact time, adsorbent dose and solution pH. Chen, Int. Lenhart, Health Hazard Evaluation Report 94–0413–2560 U.S. Department of Agriculture Animal and Plant Health Inspection Service Plant Protection and Quarantine, Fayetteville, North Carolina, 1996 Search PubMed.L. A. Iqbal, M. Cleaner Prod., 2017, 148, 958–968 CrossRef CAS.H. M. J., 2007, 133, 195–203 CrossRef CAS.Q. Chai, L. Hsu and T.-C. Eng., 2017, 5, 601–611 CrossRef CAS.H. Freundlich, Z. Eng., 2016, 4, 1407–1416 CrossRef CAS.A. Dalvand, M. 10 The operating costs. Zbair, Z. Ureña-Amate, A. This initial drop in weight (9.91%) is regularly credited to the release of water related to humidity absorbed on the surface. Nir and L. Experimental section 2.1 Adsorbent preparation JS/HSO-700 was prepared by mixing 10 g of jujube seed grounds with the appropriate quantity of H2SO4. 1e, it can be seen that with the increase in pressure, the adsorption amount increases clearly. Ji, C. 5); this indicates that intraparticle diffusion of paraquat solution onto JS/HSO-700 is not the only rate-controlling step.43 The Kip (intra-particle diffusion rate constant) values for paraquat adsorption were calculated to be 23.90, 19.45, and 20.89 mg g−1 min−1/2 at 298, 303, and 313 K, respectively. The adsorption results were better described by the pseudo-second-order kinetic model. Riley, S. The residual paraquat concentrations were determined spectrophotometrically. González-Pradas and N. Health, Part A: Environ. Adebisi, Z. 10). In the current study, the experimental results of paraquat sorption onto JS/HSO-700 were analyzed according to the most frequently used models, i.e., pseudo-first-order (PFO) and pseudo-second-order (PSO) kinetic models presented in Table 1.38,39 Table 1 Nonlinear kinetics, equilibrium adsorption models and thermodynamic equations Equations Name Description Ref. 3. Argan nut shell,25 wood sawdust,26 almond shell,27 and lignocellulose biomass are abundant in Morocco, easily available and non-toxic. The N2 adsorption isotherm of regenerated JS/HSO-700 after five cycles (without paraquat-5th-) is quite similar to that of original JS/HSO-700. Jugsujinda, J. To examine the mechanism of paraquat transfer onto the surface of JS/HSO-700, the kinetic results were analyzed using the nonlinear intraparticle diffusion model expressed by the equation presented in Table 1.41 The fitting parameters for the intraparticle kinetic model of paraquat adsorption onto JS/HSO-700 at different temperatures are given in Table 2. Eng., 2017, 5, 2740–2751 CrossRef CAS.M. Rahimdokht, E. Hameed, Y. Sonochem., 2017, 34, 343–353 CrossRef CAS PubMed.M. T. Mater., 2005, 117, 35–40 CrossRef CAS PubMed.Z. Mojović, P. Hamdi and E. Mora and J. Zhu, X. The deconvolution of the C1s spectrum (Fig. Mugadza, J. Adsorption mechanism was fully investigated based on FTIR, Raman, and BET analyses before and after adsorption. B. Ricketts, Pestic. Kennedy, C. Ojala, M. Acta, 1999, 337, 169–177 CrossRef CAS.C. Bouchelta, M. Satapathy and P. 1b) displays three peaks positioned at 531.5, 533.3, and 535.4 eV, which correspond to CO, CO, and C–OH.27,30 Fig. Eng., 2015, 3, 807–814 CrossRef CAS.T. A. Yuan, RSC Adv., 2017, 7, 13383–13389 RSC.B. Wielage, T. Pollut. Pan, Bioresour. Therefore, the operating cost for paraquat removal at these optimum operating conditions was calculated as 11.9 US$ per m3, which revealed that this adsorption process can be effectively used for the removal of paraquat onto our absorbent. Ezahri, Mater Today Chem., 2018, 8, 1–12 CrossRef.I. Anastopoulos, A. Chem, 1906, 57, 385 CAS.W. Tsai and C. He, RSC Adv., 2015, 5, 11475–11484 RSC.M. M. 2.3 Adsorption procedure The initial pH effect testing was carried out by mixing 20 mg of JS/HSO-700 and 100 mL of paraquat (100 mg L−1); the initial pH was adjusted using buffer solution (4.0–9.0). Zhou, J. Khamdahsag, N. Rahman, M. Rev. Ahmad and N. N. Based on RSM presentation, the optimum conditions for the highest removal yield of paraquat were found: pH = 6.49, CT = 25.88 min, T = 308 K and IC = 87.50 mg L−1. The model F-value was found to be 23.0493 and the P-value less than 0.05 implied that the designed model is significant.56,57 In addition, the results of ANOVA showed that the lack-of-fit was not significant; this indicates that the phenomenon was explained very well by our model with a confidence level of 95%.26,58 According to the values of the determination coefficients R2 = 0.956 (Rdj2 = 0.914), we can conclude that there is good agreement between the experimental and predicted responses of paraquat removal onto JS/HSO-700.59,60 In the same context, Fig. EPA, Exposure Factors Handbook (Final Report, 1997), U.S. Environmental Protection Agency, Washington, DC, EPA/600/P-95/002F a-c, 1216 pages, 1997 Search PubMed.D. C. Ezahri and N. These findings indicate the suitability of the Langmuir equation to describe the adsorption of paraquat onto JS/HSO-700, which is explained by monolayer adsorption of paraquat and the presence of homogenous active sites on the surface of JS/HSO-700.22,50 The obtained adsorption capacity of paraquat onto JS/HSO-700 ranged between 486.70 ± 4.47 and 851.20 ± 13.2 mg g−1. Jovanović, Chem. Debbagh-Boutarbouch, Appl. 2.2 Characterization methods XPS analysis on JS/HSO-700 was carried out using a Thermo Fisher Scientific ESCALAB 250Xi X-ray photoelectron spectroscopy system equipped with Al Kα X-ray source (hυ = 1486.7 eV) to study the chemical states of synthesized samples. It is known as Gramoxone, which is a toxic compound. Food Chem., 1990, 38, 1985–1988 CrossRef CAS.D. R. Medjram, O. The adsorption/desorption isotherm of JS/HSO-700 and the corresponding BJH pore diameter distribution curves are presented in Fig. Chen, J. Phytoremediation, 2018, 20, 831–838 CrossRef CAS PubMed.P. Fu, L. Sonochem., 2017, 38, 197–213 CrossRef PubMed.O. S. Huang, M. The peak located at 1530 cm−1 is assigned to the CC ring stretch of aromatic rings.32 The band located at 1463 cm−1 confirms the presence of CC of aromatic rings.33 The ester group (R–C–O–R–) was observed at 1386 cm−1, with –C–O– stretching at 1100 cm−1. Besides, about 97 wt% of JS/HSO-700 was recovered. Anal. S. L. Finally, these parameters were optimized by the RSM-CCD method. Sci. Omirou, J. Awang, K. The removal treatment of paraquat can occur through several processes9 such as photodegradation,10 chemical degradation,11 and microbial metabolism.12 First, the photodecomposition reactions occur within a few centimeters of the soil's surface13 and depend largely on UV intensity.14 Other studies proved that paraquat removal from aqueous solutions could be achieved, especially by adsorption on various porous materials including clays,15–18 silica gel,9 zeolites, and mesoporous materials.19 However, carbonated materials prepared from biomass are the best adsorbent materials that can be used for the treatment of heavy metals and organic pollutants. Liq., 2017, 240, 179–188 CrossRef CAS.I. Anastopoulos, I. Wang, J. The spectral peaks at 3366 cm−1 correspond to –OH functional groups. The isotherm studies were carried out by agitating 100 mL of different concentrations of paraquat (10–100 mg L−1) mixed with 20 mg of JS/HSO-700 at three temperatures (298, 303, and 313 K) and pH 6.5 for 60 min. (e) Scanning electron microscopy. Zecchina, J. 4 (a) Effect of initial solution pH (T = 298 K; Ci = 100 mg L−1; m = 20 mg). Joneidi and N. Gamha, N. 1d). Wang and Q. Kun and Y. Soc., 1916, 252, 2221–2295 CrossRef.M. Jabli, E. Narine and R. Bhatnagar, B. Ahsaine and Z. C. XPS of C1s and O1s in Fig. T. These results are confirmed by nitrogen physisorption of JS/HSO-700 after adsorption (Fig. 7a, we note that the efficacity of JS/HSO-700 decreased by 3.18% after five cycles. Ahsaine, N. Raw materials showed smooth surface morphology; after treatment with H2SO4 and thermal treatment at 700 °C for 2 hours, we observed the formation and the porosity of the surface of JS/HSO-700. Health, Part B, 2006, 41, 485–507 CrossRef PubMed.B. Singh and K. Wittayakun, Water Sci. Prayoonpokarach and J. Fig. Bhatti, N. The thermal decomposition of the jujube seed proceeded under air between 25 °C and 900 °C with a heating rate of 10 °C min−1 (using Shimadzu Instruments DTG-60 equipment). Singh, Crit. Results and discussion 3.1 Characterizations of JS/HSO-700 (a) X-ray photoelectron spectroscopy. This journal is © The Royal Society of Chemistry 2019 Chem., 1990, 102, 236–237 CrossRef.W. T. Parkpian, C. Ojala, N. S1,† we calculated the thermodynamic parameters of paraquat adsorbed onto JS/HSO-700 (Table 4). The adsorption mechanism was proposed based on solution pH, Raman, FTIR, and BET analyses after adsorption. Drif, S. Nharingo, B. Hebert and G. Brahmi, Environ. 3.10 Cost analysis: JS/HSO-700 as a low-cost adsorbent The estimated cost of the process based on experimental results of paraquat adsorption onto JS/HSO-700 is very important for its practical applications including the estimated cost of energy consumption as well as the cost of reagents (sulfuric acid). 9b, the experimental paraquat removal (%) values are very well aligned with the Henry line.62 The significance of each coefficient was determined by P-values (Table 3S†) and insignificant terms were eliminated from the model.59,61–64 Based on these results, the second-order polynomial for paraquat removal is expressed as follows:R% (paraquat) = 82.025 + 4.798XCT + 3.387XT + 2.104XIC + 5.905XpH − 2.142XCT2 − 1.278XpH2 − 2.346XCT–THere, XCT is the contact time (min), XT is the temperature (K), XIC is the initial concentration (mg L−1) and XpH is the pH. Morris, J. However, in FTIR spectra after paraquat adsorption (Fig. J., 2011, 168, 1234–1240 CrossRef CAS.U. Guyo, T. Predominantly, carbonated materials have been widely studied because they are rich in functional groups (–OH, –NH, and CO).20,21 The high adsorption capacity and efficiency of an adsorbent are mainly controlled by the presence of functional groups in the surface of the adsorbent.22 Rahman et al. Z. Guangming, Z. Makawa, M. A volume of paraquat solution (100 mL) was agitated (200 rpm) at different temperatures (298, 303, and 313 K) for different contact times (10–180 min) and the solution was centrifuged to remove the adsorbent. Ghaedi, A. The nonlinear plots of paraquat adsorption kinetics and the calculated kinetic parameters are given in Fig. Chem, 1906, 57A, 385 Search PubMed.I. Langmuir, J. H. Damin, S. Saad and H. In these new conditions, the experimental paraquat removal efficiency was found to be 96.7 ± 2.02%, whereas the value predicted by model was 94.31 ± 4.43%. Huijun, Z. They are mainly composed of suspended solids, oxidizable organic matter, inorganic salts, detergents, inhibitors, acids and bases, toxins, and colorants. Clay Sci., 2013, 83–84, 441–448 CrossRef CAS.H. Nur, A. A cost analysis performed by our team provides proof of the low operating cost using this eco-friendly material. This sharp decrease can be associated with the decomposition of the lignocellulosic structure by rupture of its macromolecular chains.31 With increasing temperature, a constant stage in TGA curves exists up to the limit of 900 °C established for the analysis. Bertarione, F. Bello, S. The experimental paraquat removal efficiency was found to be 96.7 ± 2.02%, whereas the predicted value of the model was 94.31 ± 4.43%, showing that the predicted model values are in good agreement with the experimental value. Then, the mixture was heated at 700 °C under N2 atmosphere for 2 hours. Yang, S. 1. Margiotoudis and I. Delaune and A. Finally, cost analysis was performed to confirm the cost of the adsorbent based on energy consumption and reagent costs. Huang and Y. Photochem. Introduction Currently, due to industrial development, majority of the soil contaminants originate from industrial wastewater containing organic matter and minerals, some of which are toxic; these contaminants are released in the form of solutions, suspensions, emulsions (polar molecules) or dispersions (colloids). Ok and M. Chang, J. Mol. Tsai and H. Moreover, the variation of the ID/IG ratio from 1.03 to 0.98 shows that two typical peaks of carbon with sp3 bonding and graphitic structure with sp2 hybridization participate in the adsorption mechanism of paraquat. 5 Nonlinear fit models: PFO, PSO, and IPD. However, the values of 1/n are less than 1 at all the studied temperatures, indicating chemisorption process of paraquat onto JS/HSO-700.51 Fig. Tang, Chem. AcknowledgementsThis work was supported by the University of Ibn Zohr Faculty of Sciences. Lin, Appl. Eng., 2016, 142, C4015001 CrossRef.H. J. Lu, Y. P. Geissbühler, P. DOI: 10.1039/C8RA09337G (Paper) RSC Adv., 2019, 9, 1084-1094Received 12th November 2018 , Accepted 13th December 2018First published on 9th January 2019This paper reports the removal of paraquat from an aqueous solution using prepared carbonated jujube seed (JS/HSO-700). Civ. In most cases, their composition directly depends on the type of industry from which they are released. Hosni, N. 8 (a) FTIR spectra of JS/HSO-700 after paraquat adsorption; (b) proposed adsorption mechanism of paraquat onto JS/HSO-700. Photobiol., A, 2008, 196, 143–153 CrossRef CAS.J. Weißmüller, Angew. Phys. Microbiol., 2016, 42, 245–261 CrossRef CAS PubMed.V. R. (b) Effect of contact time (temperature: 298, 303, and 313 K; Ci= 100 mg L−1; m = 20 mg; pH = 6.5). Sun, G. Djebbar, J. Wei, M. Am. Chem. 4. Cenergy in our case represents the energy consumption of the furnace and oven in US$70 and Creagents is the cost of the reagents used in US$. (f) Raman spectroscopy. Langmuir isotherm model best fitted the adsorption equilibrium data, giving maximum adsorption capacities (Qm) of 526.3, 625, and 714 mg g−1 at 298, 303, and 313 K, respectively. 3.3 Effect of contact time The effect of temperature (298, 303, and 313 K) on the adsorption of paraquat onto JS/HSO-700 was assessed at the concentration of 100 mg L−1 at pH 6.5 (Fig. 9c) for the optimization of paraquat sorption, and two variables were taken into consideration at a time.66,67 From the results of these presentations, we infer that the increase in the pH values from 4 to 6.5 increases the paraquat removal (%) significantly from 60.20 to 85%. 8a), both peaks ascribed to –OH and CC shift by +76 cm−1 and −21 cm−1, which confirms the interaction between these groups and paraquat. The peak observed at 1245 cm−1 might be assigned to C–O stretching vibrations and –CO groups are observed at 1047 cm−1. Three temperatures were examined: 298, 303, and 313 K. Guy, Soil Sci., 1982, 6, 133 Search PubMed.P. Mac Carthy and K. For all three temperature values, the plotted intra-particle diffusion model did not pass through the origin (Fig. Swaminathan and X. He, Z. Ahmad, N. J., 2011, 171, 1–8 CrossRef CAS.G. A. Bellat, J. Gholami, A. Wen and C. Stevens, J. Tahir, Ultrason. 3.8 Mechanism of paraquat adsorbed onto JS/HSO-700 The mechanism of paraquat removal was investigated based on FTIR and Raman before and after adsorption (Fig. Afr. Table 2 Kinetic model parameters (PFO, PSO, IPD) for paraquat adsorption at various temperatures T (K) Qe,exp (mg g−1) Pseudo-first-order Pseudo-second-order Qe,cal (mg g−1) K1 (min−1) R2 Qe,cal (mg g−1) K2 (g mg−1 min−1) R2 298 425.9 415.15 ± 4.09 0.200 ± 0.02 0.975 428.52 ± 1.28 0.001 ± 0.0001 0.9957 303 446.3 444.43 ± 1.54 0.552 ± 0.03 0.9988 448.91 ± 1.05 0.006 ± 0.0001 0.9996 313 487.2 485.17 ± 7.13 0.629 ± 0.03 0.9995 488.61 ± 0.51 0.008 ± 0.51 0.9998 T (K) Intraparticle diffusion model Kip (mg g−1 min−1/2) C1 (mg g−1) R2 298 23.90 ± 7.24 205.32 ± 53.70 0.5476 303 19.45 ± 9.24 276.91 ± 68.55 0.3297 313 20.89 ± 10.18 305.49 ± 75.54 0.3185 (b) Intra-particle diffusion. Wang, Z. reported capacity of 99.9 mg g−1 for activated carbon.23 Hsu and Pan utilized modified rice husk and indicated adsorption capacity of 317.7 mg g−1.24 The aim of our study is the development of a new low-cost adsorbent from biomass for adsorption applications. Response surface methodology modeling using central composite design was performed to statistically optimize the adsorption conditions. Vetenskapsakad. Sanit. Eng. Hamdan, J. TGA of jujube seeds (Fig. Mater., 2004, 112, 133–141 CrossRef CAS PubMed.X. Han, W. Technol., 2013, 10, 1349–1356 CrossRef CAS.S. Lagergren, K. A. Environ. From Fig. Hazard. Eng., 2017, 5, 1079–1088 CrossRef CAS.I. A. Razak, in Advances in Materials and Processing Technologies XV, Trans Tech Publications, 2014, vol. Iqbal, J. Miller, J. To study the mechanism of paraquat sorption onto JS/HSO-700, several nonlinear kinetic models can be used. Bensitel and R. Aziz, Chem. Banković, A. Ycalculated; (b) probability as a function of residual and (c) contour plots (2D and 3D presentations). Socías-Viciana, M. Chem. Manan, L. Jović-Jovičić and D. Khallok, H. 8b) can be summarized as follows: (i) The adsorption of paraquat molecule inside the JS/HSO-700 adsorbent (pore filling). Furthermore, when paraquat enters the soil environment, it is quickly and strongly bound to clay minerals and organic matter and becomes biologically inactive.5 The danger of pollution by paraquat is increased by its high water solubility (620 g L−1),6 having been identified in surface and drinking waters.7 For European criteria, the maximum allowed concentrations for individual pesticides in drinking water including paraquat are 0.1 μg L− 1 and 1–3 μg L− 1 for surface water.8 Consequently, the requirement to decrease the concentration of paraquat in water is a worldwide challenge as far as water pollution is concerned. Food Chem., 1990, 38, 913–918 CrossRef CAS.D. Janke, J. Soc. Rongchapo et al.19 reported adsorption capacity of 185.2 mg g−1 using NaY as an adsorbent. Lamberti and A. Kearney and G. Li, H. These parameters decreased after adsorption of paraquat, suggesting a mesopore filling mechanism along with the deposition of some functional groups of paraquat on the JS/HSO-700 surface. Conflicts of interest Authors declare that they have no conflict of interest. Massas, Int. Polprasert, R. The kinetic studies were done with 20 mg of JS/HSO-700 and an initial concentration of 100 mg L−1. S2† and 8a). The FTIR spectra of the prepared JS/HSO-700 show two principal peaks corresponding to –OH functional groups (3254 cm−1) and aromatic CC bonds (1629 cm−1). Steven and W. Qual., 1986, 15, 103–107 CrossRef CAS.G. Rytwo, S. The Brunauer–Emmett–Teller (BET) surface area (SBET) of JS/HSO-700 was determined by the nitrogen adsorption and desorption isotherms; pore size distribution and specific surface area were measured using an AUTOSORB-1 surface area and pore size analyzer at 77 K. 9 Normality test: (a) plot of raw residuals vs. Weber and J. Technol., 2007, 98, 3617–3621 CrossRef CAS PubMed.M. Zbair, K. Rintramee, S. Fig. Chem., 1906, 57, 385–471 CAS.Z. Anfar, M. Therefore, the sorption of paraquat on JS/HSO-700 is an endothermic process.54 The positive value of ΔS revealed the affinity of JS/HSO-700 for paraquat and increasing randomness at the solid–solution interface during the adsorption.55 3.7 Regeneration The regeneration of JS/HSO-700 after paraquat adsorption is conducted by thermal annealing under an N2 atmosphere. Pirilä, R. Scarano, S. Milutinović-Nikolić, J. Pyrolysis, 2008, 82, 70–77 CrossRef CAS.H. Deng, G. Appl. He and D. Surf. For example, Hsu et al.24 used modified rice husk as an adsorbent for paraquat removal and found adsorption capacity of 317.7 mg g−1. Hameed, Chem. Lampke, G. Tuzen, J. Both values are practically identical, which shows that the model-predicted values are in very good agreement with the experimentally determined values. Eng., 1963, 89, 31–60 Search PubMed.I. Langmuir, J. Sun, B. The isotherms can be assigned to type IV isotherms with H4-type hysteresis loops, suggesting a slit pore structure of JS/HSO-700. Asfaram, F. 5 and Table 2, respectively. Naciri, R.